

Surface Modification of $\text{LiNi}_{1/3}\text{Co}_{1/3}\text{Mn}_{1/3}\text{O}_2$ Hollow Nano-micro Hierarchical Microsphere with MgF_2 Coating as Cathode materials for Lithium-Ion Batteries

Jun Zhang¹, Zhu-Yuan Li², Hai-Lang Zhang^{2,*}

¹ School of Automobile and Mechanical-Electrical Engineering, Xinyang Vocational & Technical College, Xinyang 464000, Henan Province, P.R. China

² School of Chemical and Material Engineering, Jiangnan University, Wuxi 214122, Jiangsu Province, P. R.China

*E-mail: zhl8868@vip.163.com

Received: 13 November 2021 / Accepted: 19 December 2021 / Published: 2 February 2022

$\text{LiNi}_{1/3}\text{Co}_{1/3}\text{Mn}_{1/3}\text{O}_2$ hollow nano-micro hierarchical microsphere synthesized by a template-sacrificial method was modified by different contents of MgF_2 via simple chemical deposition. The lattice parameters calculated from the X-ray diffraction (XRD) patterns by Rietveld refinement reveal that MgF_2 coating does not affect the layered structure of $\text{LiNi}_{1/3}\text{Co}_{1/3}\text{Mn}_{1/3}\text{O}_2$. The MgF_2 is satisfactorily coated onto the surface of $\text{LiNi}_{1/3}\text{Co}_{1/3}\text{Mn}_{1/3}\text{O}_2$, which is confirmed by scanning electron microscopy (SEM) and energy dispersive spectroscopy (EDS) mapping. The results of galvanostatic charge/discharge experiments demonstrate that the MgF_2 coating can greatly enhance the rate performance and cycling stability of the $\text{LiNi}_{1/3}\text{Co}_{1/3}\text{Mn}_{1/3}\text{O}_2$. The 1 wt.% MgF_2 -coated $\text{LiNi}_{1/3}\text{Co}_{1/3}\text{Mn}_{1/3}\text{O}_2$ displays the most excellent electrochemical performances. It delivers an initial discharge capacity of 197.1 mAhg^{-1} at 0.1 C in the voltage of 2.5–4.6 V, and the capacity retention of 94.4% after 50 cycles at 0.2 C. The results of electrochemical impedance spectroscopy (EIS) demonstrate that the MgF_2 coating can reduce the HF erosion and the oxygen release from the highly lithium deintercalation by preventing its direct contact with the electrolyte.

Keywords: Lithium-ion battery; cathode materials; $\text{LiNi}_{1/3}\text{Co}_{1/3}\text{Mn}_{1/3}\text{O}_2$; MgF_2 coating; template-sacrificial method

1. INTRODUCTION

Lithium-ion batteries (LIBs) are the most important power sources for portable electronic products[1]. LiCoO_2 has been a popular cathode material because of its ease of production and stable cycling performance, but its low capacity ($140 \text{ mAh}\cdot\text{g}^{-1}$), toxicity of cobalt, high cost and the poor

thermal stability prohibit its use in hybrid electric vehicles (HEVs) and electric vehicles (EVs) in the future[2, 3]. Therefore, the possible cathode materials with higher specific capacity for lithium ion batteries have led to the study of researchers. Since Ohzuku first synthesized the layered cathode material $\text{LiNi}_{1/3}\text{Mn}_{1/3}\text{Co}_{1/3}\text{O}_2$, it has gradually attracted widespread attention[4]. $\text{LiNi}_{1/3}\text{Mn}_{1/3}\text{Co}_{1/3}\text{O}_2$ as one of the promising alternatives to LiCoO_2 cathode materials has been widely investigated by many researchers because of its high discharge capacity, high rate capability, long cycling ability, low cost and environmental friendliness[5-7]. However, $\text{LiNi}_{1/3}\text{Mn}_{1/3}\text{Co}_{1/3}\text{O}_2$ cathode material suffers from rapid capacity fading and inferior rate capabilities, making it difficult to meet the requirements of HEVs and EVs for higher charge and discharge rate capability of lithium ion batteries[8, 9].

To solve those issues, many researches recently have reported that surface modification as an effective way to improve the electrochemical performance of $\text{LiNi}_{1/3}\text{Mn}_{1/3}\text{Co}_{1/3}\text{O}_2$. Surface modification has the advantages of the little effect on original capacity due to no reduction of the amount of electrochemically active elements and could inhibit the side reaction between the electrolyte and the cathode material[10-12]. Therefore, a series of metal oxides, metal phosphates and metal fluoride have been used to surface coating for $\text{LiNi}_{1/3}\text{Mn}_{1/3}\text{Co}_{1/3}\text{O}_2$, such as Al_2O_3 [13], FePO_4 [14], AlF_3 [15] and so on. Among the above mentioned materials, metal fluoride is one of the most promising candidates[16]. Zhao et al.[17] reported that 1 wt.% AlF_3 and 1 wt.% MgF_2 coated $\text{LiNi}_{1/3}\text{Co}_{1/3}\text{Mn}_{1/3}\text{O}_2$ cathode materials showed an optimized electrochemical performance. It presents an initial capacity of 207.2mAh/g at 0.2 C in the voltage of 2.8-4.7 V, and has a capacity retention of 81.6% after 65 cycles, which is due to the reduction of the interface charge transfer impedance.

Recently, much more research work has been focused on the preparation methods to enhance the electrochemical properties. $\text{LiNi}_x\text{Co}_y\text{Mn}_{1-x-y}\text{O}_2$ ($x+y=1$, $x>0$, $y>0$) cathode materials were generally synthesized by co-precipitation method[18], sol-gel method[19] and solid-state method[6]. Recently, template-sacrificial method has been used to synthesize $\text{LiNi}_x\text{Co}_y\text{Mn}_{1-x-y}\text{O}_2$ ($x+y=1$, $x>0$, $y>0$) cathode materials[20,21]. Fang et al.[22] prepared hollow peanut-like hierarchical mesoporous $\text{LiNi}_{1/3}\text{Mn}_{1/3}\text{Co}_{1/3}\text{O}_2$ by a simple self-template solid-state method, which presented superior capacities and rate performances with the initial discharge capacities of 144.7 mAhg^{-1} at 10 C. Xiong et al.[23] has synthesized high-performance hierarchical $\text{LiNi}_{1/3}\text{Mn}_{1/3}\text{Co}_{1/3}\text{O}_2$ microspheres via template-sacrificial route, and the $\text{LiNi}_{1/3}\text{Mn}_{1/3}\text{Co}_{1/3}\text{O}_2$ can achieve the initial discharge capacity of 196 mAhg^{-1} at 0.1 C between 2.5-4.4 V. Their results give a clear evidence that hollow architecture is beneficial to superior electrochemical performance of cathode materials.

In our laboratory, some research work has been done for improving the electrochemical performances of cathode materials[24-27].

Nevertheless, researchers have only used this method to synthesize pristine cathode materials, and have not done further modification research. In this work, $\text{LiNi}_{1/3}\text{Mn}_{1/3}\text{Co}_{1/3}\text{O}_2$ cathode materials have been synthesized via a simple template-sacrificial method, and the effect of MgF_2 coating on the physical and the electrochemical properties have been investigated.

2. EXPERIMENTAL

2.1 Sample preparation

The $\text{LiNi}_{1/3}\text{Mn}_{1/3}\text{Co}_{1/3}\text{O}_2$ cathode materials was synthesized by template-sacrificial method and firing at 850 °C in air for 12 h as our previous report[24]. For preparing the MgF_2 -coated sample, firstly the $\text{Mg}(\text{NO}_3)_2 \cdot 6\text{H}_2\text{O}$ and NH_4F were dissolved in deionized water, respectively, the as-prepared $\text{LiNi}_{1/3}\text{Mn}_{1/3}\text{Co}_{1/3}\text{O}_2$ sample was added to the $\text{Mg}(\text{NO}_3)_2$ solution and stirred for 30 min. Then, the NH_4F solution was added dropwise and stirred at 80 °C until all the deionized water had evaporated completely. Finally the obtained powders were heated at 400 °C for 5 h in air. The samples modified with 0.5, 1 and 3wt.% MgF_2 were remarked as 0.5 wt.%- MgF_2 , 1 wt.%- MgF_2 , and 3 wt.%- MgF_2 , respectively.

2.2 Physical characterizations

Power X-ray diffraction (XRD, Advanced D8, Bruker) using $\text{Cu-K}\alpha$ radiation was employed to characterized the crystalline phase and structure of synthesized materials. The XRD data were collected from 10° to 90° in 2θ with a scanning rate of 2° min^{-1} . The morphology of the samples was analyzed by scanning electron microscope (SEM, S4800, Hitachi) and energy dispersive spectroscopy (EDS) mapping.

2.3 Electrochemical characteristics

The electrochemical performances of as-prepared materials were measured by CR2032 type coin cells, which consist of a lithium metal anode and cathode separated by Celgard 2325 porous polypropylene. The cathode electrodes were prepared by mixing active material (80wt.%), acetylene back (12wt.%) and polyvinylidene fluoride (PVDF, 8wt.%) in N-methylpyrrolidone (NMP), then the mixture-slurry was coated onto Al foil and dried at 80 °C for 12 h in a vacuum oven. The electrolyte used was a 1M LiPF_6 dissolved in the mixture of carbonate (EC) with dimethyl carbonate (DMC) and diethyl carbonate (DEC) (1:1:1 by volume). The coin cells were assembled in an Ar-filled dry glove box (Mikrouna SUPER 1220/750, Shanghai, China), and were galvanostatic charged / discharged at different rates (1 C = 180 mAhg^{-1}) in the voltage range of 2.5-4.6V (vs. Li^+/Li) on a Land Battery Tester (Wuhan, China). In addition, the electrochemical impedance spectroscopy (EIS) of coin cells were conducted by electrochemical work station (IM6, Germany). The EIS measurements were performed over frequency from 0.01 Hz to 100k Hz with amplitude of 5 mV.

3. RESULTS AND DISCUSSION

3.1 Physical characteristics

XRD patterns of the MgF_2 -coated $\text{LiNi}_{1/3}\text{Co}_{1/3}\text{Mn}_{1/3}\text{O}_2$ cathode materials are given in Fig. 1. It shows that all the samples are confirmed to be well-defined hexagonal $\alpha\text{-NaFeO}_2$ with R-3m space group.

The well resolved planes of (006)/(102) and (108)/(110) peaks indicate all samples possess a typical hexagonal layered structure[28]. No diffraction peaks can be assigned to the MgF_2 phase, which may be due to low content or that they were non-crystallized at 400 °C. In order to subdivide the difference in structural parameters of the pristine and MgF_2 -coated $\text{LiNi}_{1/3}\text{Co}_{1/3}\text{Mn}_{1/3}\text{O}_2$, Rietveld refinement is performed to obtain the structural parameters of all samples, and the results are shown in Table 1. As shown in Table 1, the lattice parameters (a , c and V) of MgF_2 -coated $\text{LiNi}_{1/3}\text{Co}_{1/3}\text{Mn}_{1/3}\text{O}_2$ cathode materials are very close to that of the pristine $\text{LiNi}_{1/3}\text{Co}_{1/3}\text{Mn}_{1/3}\text{O}_2$, which demonstrate that the layered structure does not change after coating the $\text{LiNi}_{1/3}\text{Co}_{1/3}\text{Mn}_{1/3}\text{O}_2$ with MgF_2 [29]. Besides, the $I_{(003)}/I_{(104)}$ value reveals the degree of cation mixing. As the results show, the values of the pristine and MgF_2 -coated $\text{LiNi}_{1/3}\text{Co}_{1/3}\text{Mn}_{1/3}\text{O}_2$ were larger than 1.2 and are very close to each other, which indicate that the all samples have low cation mixing. The ratio of c/a in the XRD patterns is always used to indicate the extent of trigonal distortion, and a higher value of c/a usually means the more perfect hexagonal layered structure. The c/a ratios of all samples are higher than 4.9, which means that they all have the excellent hexagonal ordering[30].

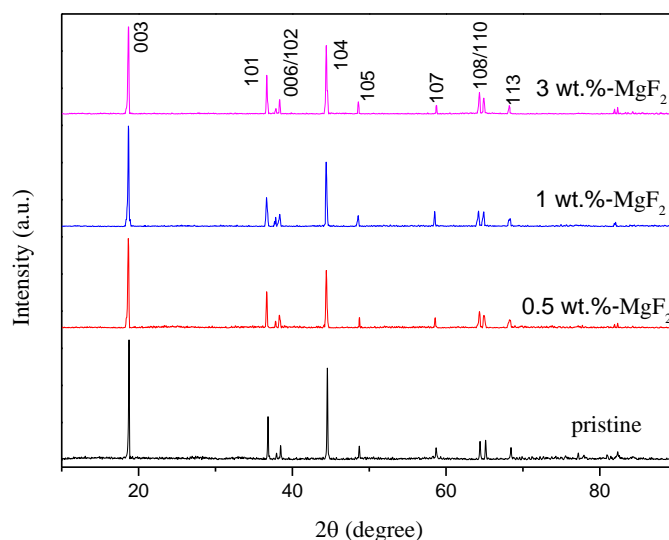


Figure 1. XRD patterns of the pristine and MgF_2 -coated $\text{LiNi}_{1/3}\text{Mn}_{1/3}\text{Co}_{1/3}\text{O}_2$ cathode materials

Table 1. Refined lattice parameters of the pristine and MgF_2 -coated $\text{LiNi}_{1/3}\text{Mn}_{1/3}\text{Co}_{1/3}\text{O}_2$ cathode materials

| Sample (wt.%) | $a(\text{Å})$ | $c(\text{Å})$ | c/a | $I_{(003)}/I_{(104)}$ | $V(\text{Å}^3)$ |
|---------------|---------------|---------------|--------|-----------------------|-----------------|
| pristine | 2.8605 | 14.2267 | 4.9735 | 1.3263 | 100.88 |
| 0.5 | 2.8605 | 14.2269 | 4.9736 | 1.3262 | 100.88 |
| 1 | 2.8604 | 14.2265 | 4.9736 | 1.3260 | 100.89 |
| 3 | 2.8602 | 14.2266 | 4.9739 | 1.3264 | 100.89 |

The SEM images of the pristine and MgF_2 -coated $\text{LiNi}_{1/3}\text{Mn}_{1/3}\text{Co}_{1/3}\text{O}_2$ cathode materials are presented in Fig. 2.

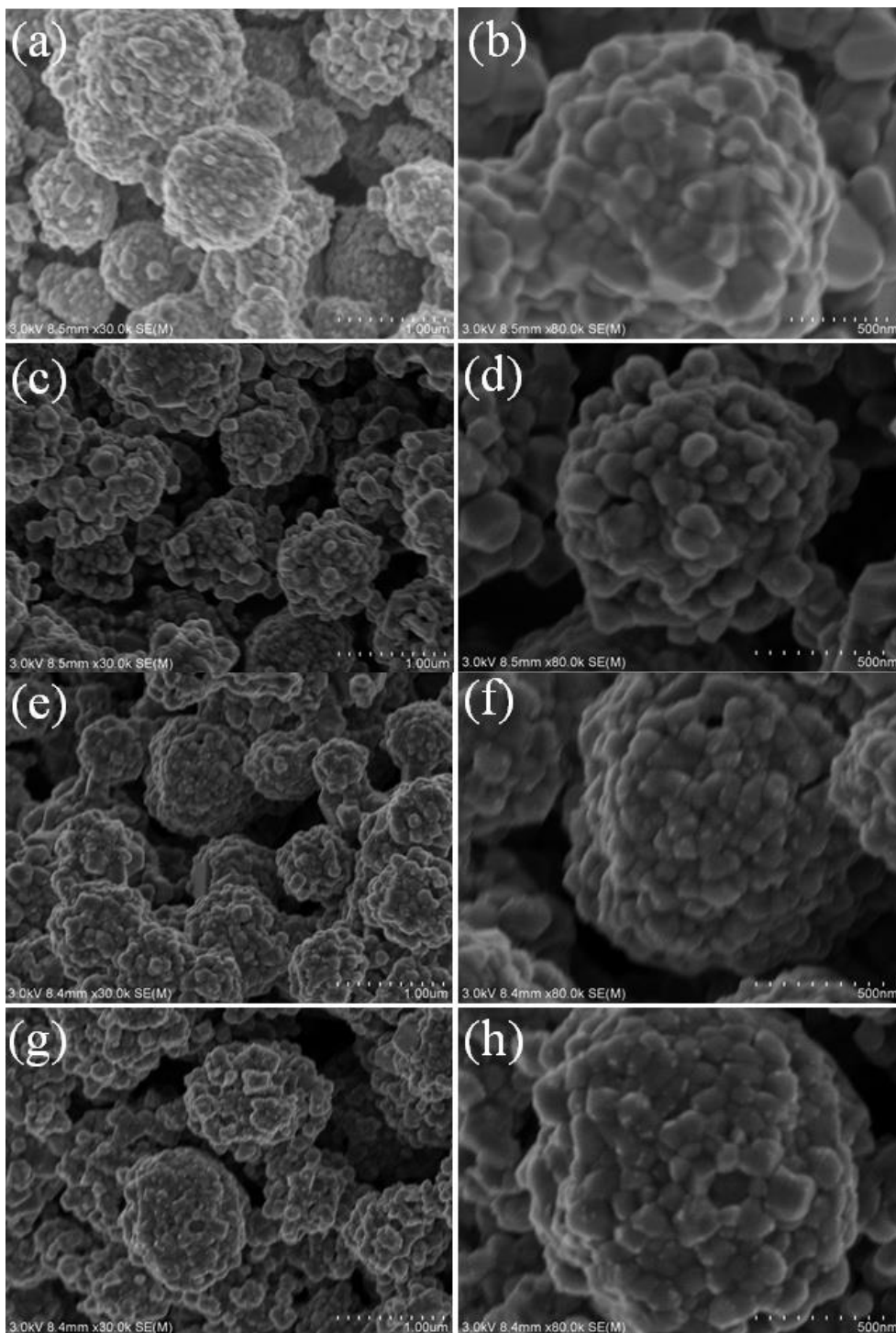


Figure 2. SEM images of the pristine and MgF_2 -coated $\text{LiNi}_{1/3}\text{Mn}_{1/3}\text{Co}_{1/3}\text{O}_2$ cathode materials: (a)-(b) pristine, (c)-(d) 0.5 wt.-%- MgF_2 , (e)-(f) 1wt.-%- MgF_2 , (g)-(h) 3wt.-%- MgF_2

As it can be seen, the morphology of samples is controlled by using MnO_2 hollow microspheres, and the microspheres are well preserved during the template-sacrificial process. It is revealed that the pristine $\text{LiNi}_{1/3}\text{Mn}_{1/3}\text{Co}_{1/3}\text{O}_2$ is composed of approximately 100 nm to 200 nm primary nanoparticles, with smooth surface and clear boundaries. With the increase of the coating amount of MgF_2 , the microspherical appearance of MgF_2 -coated $\text{LiNi}_{1/3}\text{Mn}_{1/3}\text{Co}_{1/3}\text{O}_2$ did not change, but nano-scale particles

appeared gradually on the surface of the microspheres, and the number of particles increased with the increase of the coating amount. In order to observe the detailed existence of MgF_2 on the surface, EDS testing was performed. As shown in Fig. 3, the elements of O, Mg, Mn, Co and Ni are homogeneously distributed in 1 wt.% MgF_2 -coated $\text{LiNi}_{1/3}\text{Co}_{1/3}\text{Mn}_{1/3}\text{O}_2$ structure surface. The element of F is not detected because of that the F element is ultra-light element with a low content, but the mapping of Mg can indicates that MgF_2 is homogeneously distributed on the surface of $\text{LiNi}_{1/3}\text{Mn}_{1/3}\text{Co}_{1/3}\text{O}_2$ cathode materials.

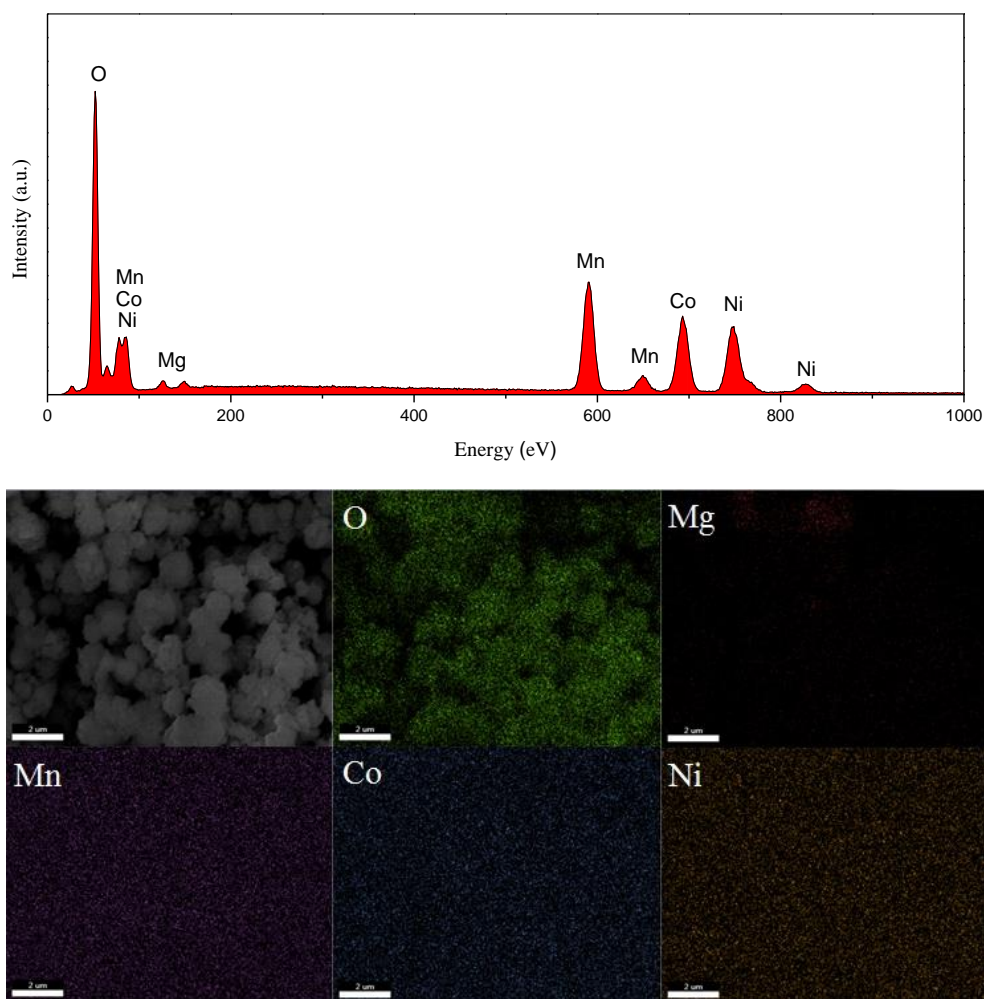


Figure 3. EDS element mappings of 1 wt.% MgF_2 -coated $\text{LiNi}_{1/3}\text{Co}_{1/3}\text{Mn}_{1/3}\text{O}_2$

3.2 Electrochemical characteristics

The typical initial charge/discharge curves of the pristine and MgF_2 -coated $\text{LiNi}_{1/3}\text{Mn}_{1/3}\text{Co}_{1/3}\text{O}_2$ cathode materials at 0.1 C in the voltage range of 2.5-4.6 V are shown in Fig.4. The initial discharge capacity of the pristine and 0.5 wt.%, 1 wt.% 3 wt.% MgF_2 -coated $\text{LiNi}_{1/3}\text{Mn}_{1/3}\text{Co}_{1/3}\text{O}_2$ is 203.9 mAh g^{-1} , 201.4 mAh g^{-1} , 197.1 mAh g^{-1} and 190.4 mAh g^{-1} , respectively. It can be seen that the initial discharge of the $\text{LiNi}_{1/3}\text{Mn}_{1/3}\text{Co}_{1/3}\text{O}_2$ show a gradual decrease with the increase of the MgF_2 coating amount, which

is due to the fact that the MgF_2 coating layer is not electrochemically active. Significantly, the capacity loss of the pristine and MgF_2 -coated $\text{LiNi}_{1/3}\text{Mn}_{1/3}\text{Co}_{1/3}\text{O}_2$ materials during initial charge/discharge is 40.3 mAh g^{-1} , 38.9 mAh g^{-1} (0.5 wt.%), 34.8 mAh g^{-1} (1 wt.%) and 42.7 mAh g^{-1} (3 wt.%), respectively, which indicate that an appropriate amount of MgF_2 coating can reduce the irreversible capacity of $\text{LiNi}_{1/3}\text{Mn}_{1/3}\text{Co}_{1/3}\text{O}_2$ during the initial charge/discharge significantly.

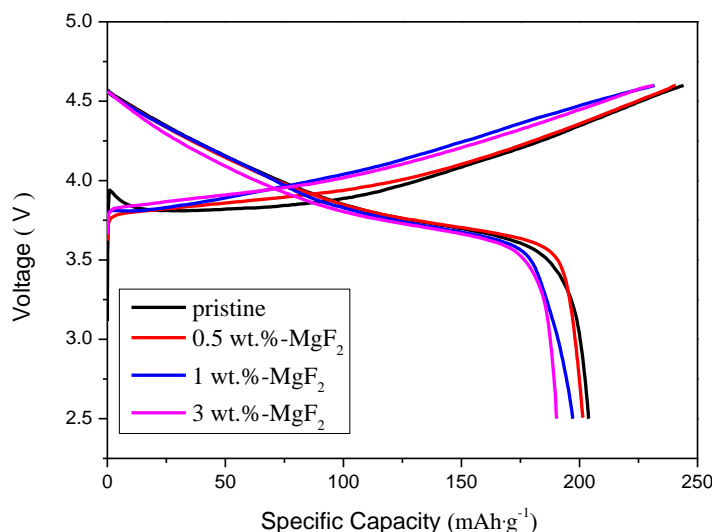


Figure 4. Initial charge/discharge curves of pristine and MgF_2 -coated $\text{LiNi}_{1/3}\text{Mn}_{1/3}\text{Co}_{1/3}\text{O}_2$ cathode materials at 0.1 C in the voltage range of 2.5-4.6 V

Fig.5 (a) presents the specific capacities of pristine and MgF_2 -coated $\text{LiNi}_{1/3}\text{Mn}_{1/3}\text{Co}_{1/3}\text{O}_2$ at different discharge rates between 2.5-4.6 V. The current densities used for the test increase from 0.1 C to 5 C and then back to 0.1 C, and 10 cycles of charge/discharge per current density. It can be seen that all the samples deliver decreased capacities with increasing current density due to the limited diffusion rate of charge in the electrodes[31]. The pristine sample shows a higher discharge capacity than that of MgF_2 -coated samples at 0.1 C. However, the 0.5 wt.% and 1 wt.% MgF_2 -coated $\text{LiNi}_{1/3}\text{Mn}_{1/3}\text{Co}_{1/3}\text{O}_2$ exhibits higher discharge capacities than $\text{LiNi}_{1/3}\text{Mn}_{1/3}\text{Co}_{1/3}\text{O}_2$ at 1 C and 5 C. In details, the 1 wt.% MgF_2 -coated $\text{LiNi}_{1/3}\text{Mn}_{1/3}\text{Co}_{1/3}\text{O}_2$ exhibits 119.1 mAh g^{-1} while the pristine $\text{LiNi}_{1/3}\text{Mn}_{1/3}\text{Co}_{1/3}\text{O}_2$ only delivers 108.9 mAh g^{-1} at 5 C. While the rate recovers to 0.1 C, the discharge capacities of the pristine, 0.5 wt.% and 1 wt.% MgF_2 -coated $\text{LiNi}_{1/3}\text{Mn}_{1/3}\text{Co}_{1/3}\text{O}_2$ are increased to 190.9 mAh g^{-1} , 188.2 mAh g^{-1} and 191.4 mAh g^{-1} , respectively. Appropriate amount of MgF_2 -coated $\text{LiNi}_{1/3}\text{Mn}_{1/3}\text{Co}_{1/3}\text{O}_2$ exhibits better rate performance than the pristine sample, which is mainly due to the coating MgF_2 can reduce the side reaction between material and electrolyte, resulting in lower electrochemical impedance. However, the rate capability of 3 wt.% MgF_2 -coated $\text{LiNi}_{1/3}\text{Mn}_{1/3}\text{Co}_{1/3}\text{O}_2$ is worse than that of the pristine sample, which is mainly due to the higher content of coating MgF_2 will impede the diffusion of Li^+ and reduce the electronic conductivity.

To further evaluate the superiority of the MgF_2 -coated $\text{LiNi}_{1/3}\text{Mn}_{1/3}\text{Co}_{1/3}\text{O}_2$ cathode material, the battery was tested for cyclic charge/discharge at 0.2 C in the voltage range of 2.5-4.6V, and the results

are shown in Fig.5 (b). As it can be seen, the initial discharge capacity of the pristine $\text{LiNi}_{1/3}\text{Mn}_{1/3}\text{Co}_{1/3}\text{O}_2$ is 196.1 mAh g^{-1} , and the discharge capacity of material is only 176.7 mAh g^{-1} with 90.1% capacity retention after 50 cycles. Although the values of the discharge specific capacity of the 0.5 wt.% and 1 wt.% MgF_2 -coated $\text{LiNi}_{1/3}\text{Mn}_{1/3}\text{Co}_{1/3}\text{O}_2$ are 195.1 mAh g^{-1} and 190.7 mAh g^{-1} , respectively, they exhibit better cycling stability with 91.8% and 94.4% capacity retention after 50 cycles, respectively. It is worth noting that the 3 wt.% MgF_2 -coated $\text{LiNi}_{1/3}\text{Mn}_{1/3}\text{Co}_{1/3}\text{O}_2$ illustrates lower discharge capacity in the first cycle and after 80 cycles, but the capacity retention is 91.6% after 50 cycles. The reason may be that MgF_2 coating is not an electrode active material and more coating may deteriorate the electrochemical properties.

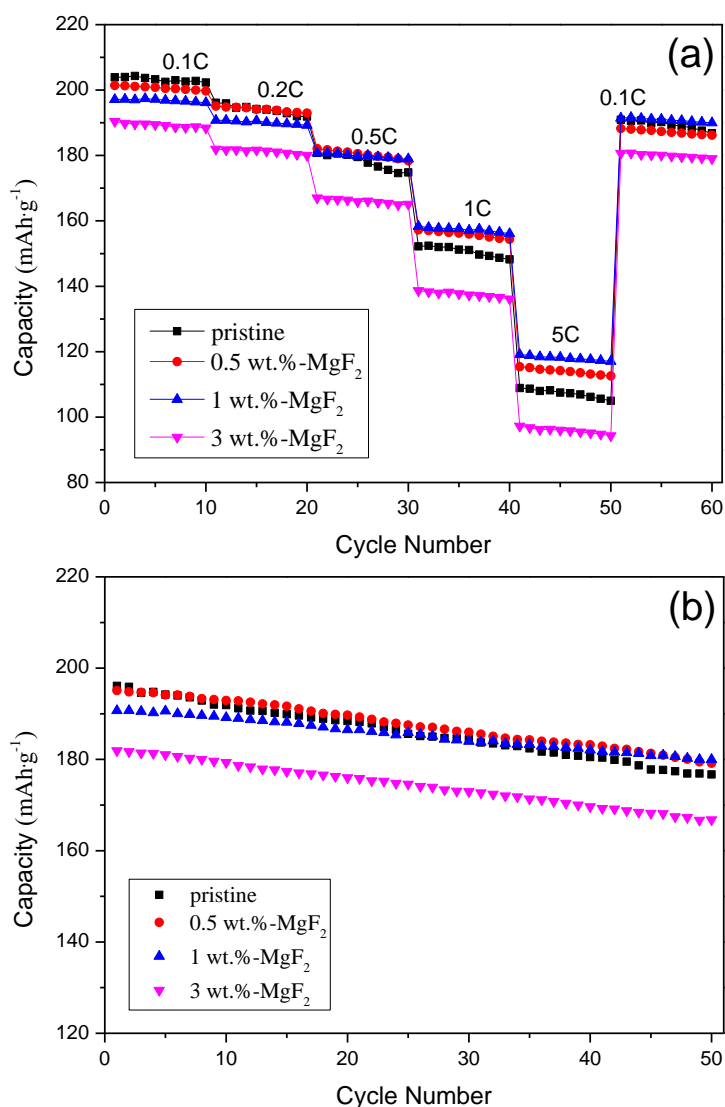


Figure 5. (a) The rate performance, (b) the cycle performance of pristine and MgF_2 -coated $\text{LiNi}_{1/3}\text{Mn}_{1/3}\text{Co}_{1/3}\text{O}_2$ cathode materials in the voltage range of 2.5-4.6 V

The results illustrate that appropriate amount of MgF_2 -coated $\text{LiNi}_{1/3}\text{Mn}_{1/3}\text{Co}_{1/3}\text{O}_2$ not only improves material rate performance but also presents excellent cycling stability, which may be : (1) Appropriate amount of MgF_2 coating can avoid direct contact between material and electrolyte, relieve

electrolyte corrosion and SEI film growth rate. (2) Appropriate amount of MgF_2 coating can improve the structural stability of the material and reduce the growth rate of internal cracks in the material particles.

In order to further study the differences in electrochemical performances of the pristine and 1 wt.% MgF_2 -coated $\text{LiNi}_{1/3}\text{Mn}_{1/3}\text{Co}_{1/3}\text{O}_2$, the electrochemical impedance spectroscopy (EIS) of two samples were tested, which is a main tool to analyze kinetic process of Li^+ intercalation and deintercalation into electrode materials[32]. Fig. 6 presents the EIS profiles of the pristine and 1 wt.% MgF_2 -coated $\text{LiNi}_{1/3}\text{Mn}_{1/3}\text{Co}_{1/3}\text{O}_2$ after 5 and 50 cycles at 0.2 C between 2.5 to 4.6 V. Both the two plots contain a semicircle in the high frequency, a semicircle in mid-low frequency and a straight line in the low frequency, corresponding to the impedance for a solid electrolyte interface layer (R_{sei}), the surface charge transfer resistance (R_{ct}) and the resistance of Li^+ diffusion in the crystal lattice.

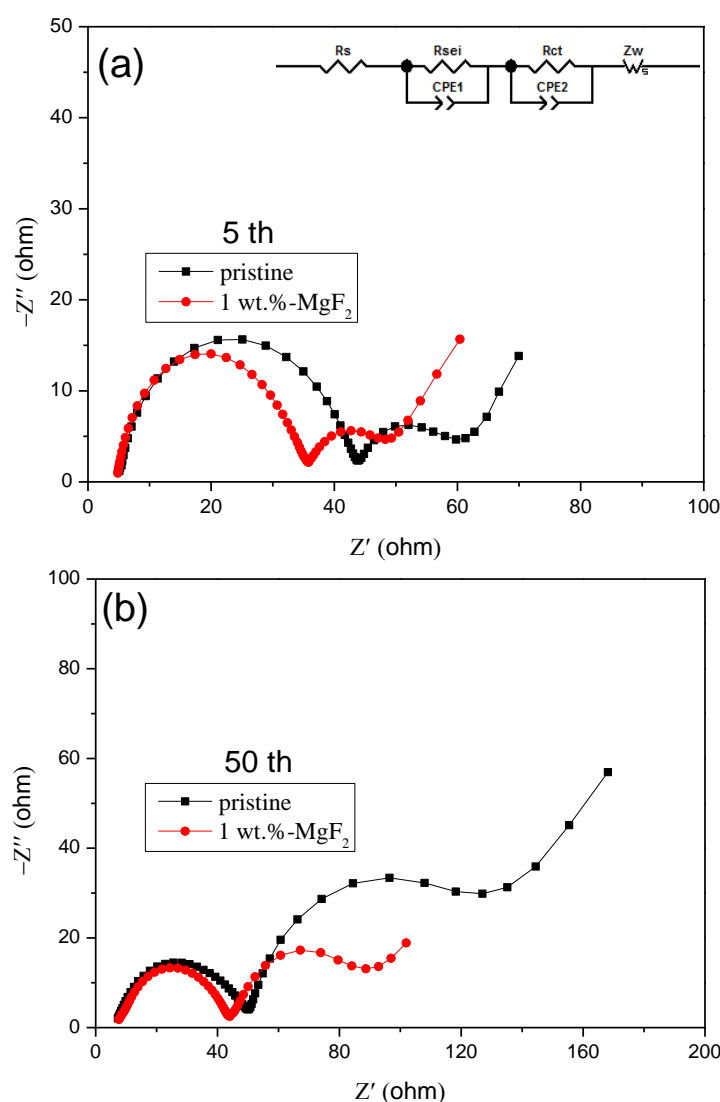


Figure 6 Nyquist plots of pristine and 1 wt.% MgF_2 -coated $\text{LiNi}_{1/3}\text{Mn}_{1/3}\text{Co}_{1/3}\text{O}_2$ cathode materials after 5 (a) and 50 (b) cycles. Inset: Equivalent circuit.

The intercept of the high frequency region and the Z' axis is mainly electrolyte (R_s)[33]. All the sections correspond to the partitions in the equivalent circuit, which is used to fit the EIS profiles to give a quantitative result to further study the effect of MgF_2 coating. The detailed values of impedance parameters could be obtained from fitting result, which were shown in Table 2. As it can be seen, the values of R_s for the pristine and 1 wt.% MgF_2 -coated $LiNi_{1/3}Mn_{1/3}Co_{1/3}O_2$ have almost no change after 5 and 50 cycles. The R_{sei} of 1 wt.% MgF_2 -coated $LiNi_{1/3}Mn_{1/3}Co_{1/3}O_2$ is lower than that of the pristine sample after 5 and 50 cycles, which indicates that the formation of the SEI layer is suppressed by the MgF_2 coating. The R_{ct} value of 1 wt.% MgF_2 -coated $LiNi_{1/3}Mn_{1/3}Co_{1/3}O_2$ increases from 12.44 Ω after 5 cycles to 44.65 Ω after 50 cycles, while that of the pristine sample increases from 17.52 Ω after 5 cycles to 92.69 Ω after 50 cycles. This increase in impedance during cycling is primarily due to the side reactions between material and electrolyte. The results demonstrate that the MgF_2 coating can reduce the HF erosion and the oxygen release from the highly lithium deintercalation by preventing its direct contact with the electrolyte. Therefore, the excellent rate performance and cycling stability of $LiNi_{1/3}Mn_{1/3}Co_{1/3}O_2$ are obtained after coating an appropriate amount of MgF_2 on the surface.

Table 2. Impedance parameters calculated based on equivalent circuit

| sample | 5th | | | 50th | | |
|-----------------|---------------|-------------------|------------------|---------------|-------------------|------------------|
| | $R_s(\Omega)$ | $R_{sei}(\Omega)$ | $R_{ct}(\Omega)$ | $R_s(\Omega)$ | $R_{sei}(\Omega)$ | $R_{ct}(\Omega)$ |
| pristine | 5.11 | 38.69 | 17.52 | 7.31 | 42.45 | 92.69 |
| 1 wt.%- MgF_2 | 4.84 | 31.01 | 12.44 | 7.65 | 36.43 | 44.65 |

4. CONCLUSIONS

MgF_2 -coated $LiNi_{1/3}Mn_{1/3}Co_{1/3}O_2$ hollow nano-micro hierarchical microsphere materials have been successfully synthesized and characterized for its structural characteristics and electrochemical performances. The 1 wt.% MgF_2 -coated $LiNi_{1/3}Mn_{1/3}Co_{1/3}O_2$ exhibited a remarkably enhanced cycling stability and rate capability between 2.5 and 4.6 V. The results of EIS indicated that MgF_2 coating layer can reduce the increase of the cathode materials during cycling.

References

1. P. He, H. J. Yu, D. Li, H. S. Zhou, *J. Mater. Chem.*, 22(2012) 3680.
2. H. J. Lee, Y. J. Park, *Solid State Ionics*, 230 (2013) 86.
3. Y. Bai, K. Jiang, S. Sun, Q. Wu, X. Lu, N. Wan, *Electrochim. Acta*, 134 (2014) 347.
4. T. Ohzuku, Y. Makimura, *Chem. Lett.*, 30 (2001) 744.
5. R. Zhang, L. W. Huang, W. Li, J. T. Liao, P. Zeng, X. L. Zhang, Y. G. Chen, *Int. Electrochem., Sci.* 13 (2018) 2248.
6. L. Tan, H. W. Liu, *Solid State Ionics*, 181 (2010) 1530.
7. Q. Q. Jiang, N. Chen, D. D. Liu, S. T. Wang, H. Zhang, *Nanoscale*, 8 (2016) 11234.
8. F. Wu, M. Wang, Y. F. Su, L. Y. Bao, S. Chen, *J. Power Sources*, 195 (2010) 2362.
9. Q. N. Sa, E. Gratz, M. N. He, W. Q. Lu, D. Apelian, Y. Wang, *J. Power Sources*, 282 (2015) 140.

10. E. Billy, M. Joulié, R. Laucournet, A. Boulineau, E. D. Vito, D. Meyer, *ACS Appl. Mater. Interfaces*, 10 (2018) 16424.
11. H. Nara, K. Morita, D. Mukoyama, T. Yokoshima, T. Momma, T. Osaka, *Electrochim. Acta*, 241 (2017) 323.
12. X. Y. Qiu, Q. C. Zhuang, Q. Q. Zhang, R. Cao, Y. H. Qiang, P. Z. Ying, S. G. Sun, *J. Electroanal. Chem.*, 687 (2012) 35.
13. K. Araki, N. Taguchi, H. Sakaebe, K. Tatsumi, Z. Ogumi, *J. Power Sources*, 269 (2014) 236.
14. X. Z. Liu, H. Q. Li, E. Yoo, M. Ishida, H. S. Zhou, *Electrochim. Acta*, 83 (2012) 253.
15. H. Y. Wang, A. D. Tang, K. L. Huang, S. Q. Liu, *Trans. Nonferrous Met. Soc. China*, 20 (2010) 803.
16. S. W. Sun, N. Wan, Q. Wu, X. P. Zhang, D. Pan, Y. Bai, X. Lu, *Solid State Ionics*, 278 (2015) 85.
17. F.F. Zhao, D. B. Mu, X.X. Hou, L. Wang, Y. H. Ren, *Adv. Mater. Res.*, 1088 (2015) 327.
18. K. Yin, W. M. Fang, B. H. Zhong, X. D. Guo, Y. Tang, X. Nie, *Electrochim. Acta*, 85 (2012) 99.
19. S. W. Lee, H. Kim, M. S. Kim, H. C. Youn, K. Kang, B. W. Cho, K. C. Roh, K. B. Kim, *J. Power Sources*, 315 (2016) 261.
20. J. L. Li, C. B. Cao, X. Y. Xu, Y. Q. Zhu, R. M. Yao, *J. Mater. Chem. A*, 38 (2013) 11848.
21. Z. Chen, J. Wang, D. L. Chao, T. Baikie, L. Y. Bai, S. Chen, Y. L. Zhao, T. C. Sum, J. Y. Lin, Z. X. Shen, *Sci. Rep.*, 6 (2016) 25771.
22. Y. C. Fang, Y. D. Huang, W. Tong, Y. J. Cai, X. C. Wang, Y. Guo, D. Z. Jia, J. Zong, *J. Alloys Comp.*, 743 (2018) 707.
23. W. Xiong, Y. Jiang, Z. Yang, D. G. Li, Y. H. Huang, *J. Alloys Comp.* 589 (2014) 615.
24. Z. Y. Li, H. L. Zhang, *Int. Electrochem. Sci.*, 14 (2019) 3524.
25. W. Yang, H. L. Zhang, *Int. Electrochem. Sci.*, 8 (2013) 11606.
26. H. L. Zhang, F. J. Wu, *Int. Electrochem. Sci.*, 15 (2020) 7417.
27. X. M. Wang, H. L. Zhang, *Int. Electrochem. Sci.* 16 (2021) 151011.
28. T. Tang, H. L. Zhang, *Electrochim. Acta*, 191 (2016), 263.
29. S. K. Hu, G. H. Cheng, M. Y. Cheng, B. J. Hwang, R. Santhanam, *J. Power Sources*, 188 (2009) 564.
30. L. L. Zhang, J. Q. Wang, X. L. Yang, G. Liang, T. Li, P. L. Yu, D. Ma, *ACS Appl. Mater. Interfaces*, 10 (2018) 11663.
31. L. L. Xiong, M. T. Sun, Y. L. Xu, X. F. Du, X. Xiao, *Solid State Ionics*, 325 (2018) 170.
32. Y. H. Li, J. Y. Liu, Y. K. Lei, C. Y. Lai, Q. J. Xu, *J. Mater. Sci.*, 52 (2017) 13596.
33. X. Z. Liu, P. He, H. Q. Li, M. Ishida, H. S. Zhou, *J. Alloys Comp.*, 552 (2013) 76.